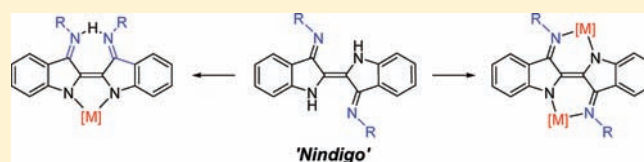


Redox-Active Bridging Ligands Based on Indigo Diimine (“Nindigo”) Derivatives

Graeme Nawn,[†] Kate M. Waldie,[†] Simon R. Oakley,[†] Brendan D. Peters,[†] Derek Mandel,[†] Brian O. Patrick,[‡] Robert McDonald,[§] and Robin G. Hicks^{*,†}[†]Department of Chemistry, University of Victoria, P.O. Box 3065 STN CSC, Victoria, British Columbia V8W 3V6, Canada[‡]Crystallography Laboratory, Department of Chemistry, University of British Columbia, Vancouver, British Columbia V6T 1Z3, Canada[§]Crystallography Laboratory, Department of Chemistry, University of Alberta, 11227 Saskatchewan Drive NW, Edmonton, Alberta T6G 2G2, Canada

S Supporting Information

ABSTRACT: Reactions of indigo with a variety of substituted anilines produce the corresponding indigo diimines (“Nindigos”) in good yields. Nindigo coordination complexes are subsequently prepared by reactions of the Nindigo ligands with Pd(hfac)₂. In most cases, binuclear complexes are obtained in which the deprotonated Nindigo bridges two Pd(hfac) moieties in the expected bis-bidentate binding mode. When the Nindigo possesses bulky substituents on the imine (mesityl, 2,6-dimethylphenyl, 2,6-diisopropylphenyl, etc.), mononuclear Pf(hfac) complexes are obtained in which the Nindigo core has isomerized from a *trans*- to a *cis*-alkene; in these structures, the palladium is bound to the *cis*-Nindigo ligand at the two indole nitrogen atoms; the remaining proton is bound between the imine nitrogen atoms. The palladium complexes possess intense electronic absorption bands [near 920 nm for the binuclear complexes and 820 nm for the mononuclear *cis*-Nindigo complexes; extinction coefficients are $(1.0\text{--}2.0) \times 10^4 \text{ M}^{-1} \text{ cm}^{-1}$] that are ligand-centered ($\pi\text{--}\pi^*$) transitions. Cyclic voltammetry investigations reveal multiple redox events that are also ligand-centered in origin. All of the palladium complexes can be reversibly oxidized in two sequential one-electron steps; the binuclear complexes are reduced in a two-electron process whose reversibility depends on the Nindigo ligand substituent; the mononuclear palladium species show two one-electron reductions, only the first of which is quasi-reversible.



INTRODUCTION

Redox-active ligands (RALs, also known as noninnocent¹ ligands) mimic two common characteristics of transition metals: the ability to adopt more than one charge (oxidation) state and the ability to support an open-shell configuration in one or more of their accessible oxidation states. Complexes containing RALs and electroactive metal ions have been the focus of long-standing investigations of their fundamental electronic structure. Additionally, RALs have been found to be prevalent in several domains of bioinorganic chemistry,² and the relatively recent spate of publications that exploit RAL complexes in stoichiometric and catalytic transformations³ highlight a resurgence of interest in these types of compounds.⁴

Most RALs bind to a single metal ion. Somewhat less common are RALs that are capable of bridging two or more metal ions. There are a number of features that distinguish bridging RALs from their more familiar monometallic counterparts. Metal–metal “communication” in the context of mixed valency has long been a central theme in multimetallic chemistry, and the introduction of a redox-active linker provides an intriguing twist (and an additional degree of complexity) on metal–metal electronic interactions.^{5,6} Moreover, spectacular solid-state properties such as high conductivity⁷ or magnetic ordering⁸ can be realized in

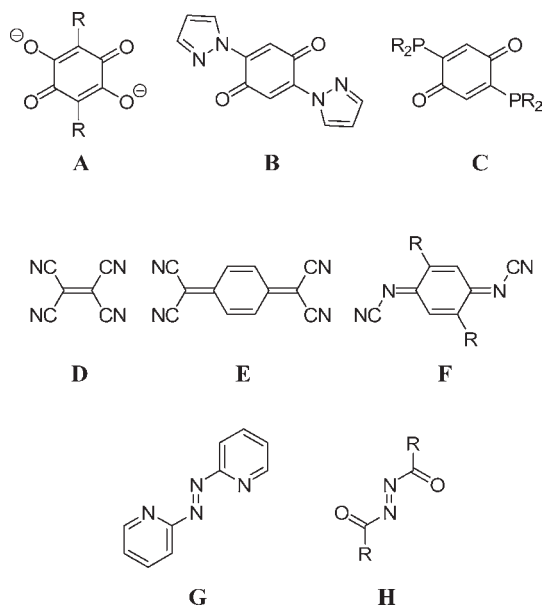
polymeric assemblies (coordination polymers and networks) based on bridging RALs. Finally, the reactivity of bridging RAL complexes is essentially unexplored, but it is not unreasonable to imagine chemical applications based on multiple redox-active units acting in concert. Several metalloenzyme active sites are based on multimetallic complexes in which cooperativity between several redox-active metal ions empowers unique redox chemistry (e.g., 4Fe ferredoxins,⁹ nitrogenase Fe₇Mo cofactor,¹⁰ and the Mn₄ oxygen-evolving complex of PSII,¹¹ to name a few).

Examples of common classes of bridging RALs are depicted below. Probably the best known are bis-chelating *p*-dioxolenes (*p*-quinones), as analogues of the ubiquitous *o*-dioxolenes. Derivatives of the (deprotonated) 2,5-dihydroxybenzoquinone system (“anilates”) A were initially popular as structural linkers,¹² but the redox activity of these species, and their nitrogen-based analogues,¹³ as coordinated ligands has received recent attention.¹⁴ Other examples include bis(pyrazolyl)benzoquinone B¹⁵ and bis(phosphine) quinones C.^{5,16} A second major class is comprised of the conjugated polynitriles tetracyanoethylene D,⁸ 7,7,8,8-tetracyanoquinodimethane E,¹⁷ and *N,N'*-dicyanoquinonediimine F;¹⁸ all are excellent

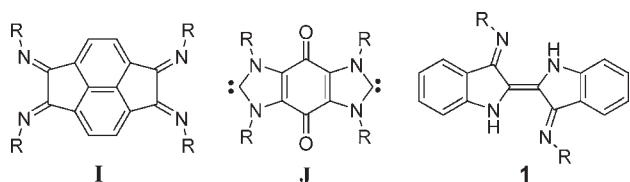
Received: February 24, 2011

Published: June 20, 2011

electron acceptors and can bind multiple metal ions via the nitrile donors.¹⁹ A third group is based on the so-called “S-frame” ligands based on the reducible azo functionality (G and H) popularized by Kaim.²⁰ Finally, some nitrogen-rich heterocyclic ligands, e.g., 2,2'-bipyrimidine,²¹ substituted *s*-tetrazines,²² and pyrazines,²³ can be reduced to radical anions and dianions in selected coordination complexes.

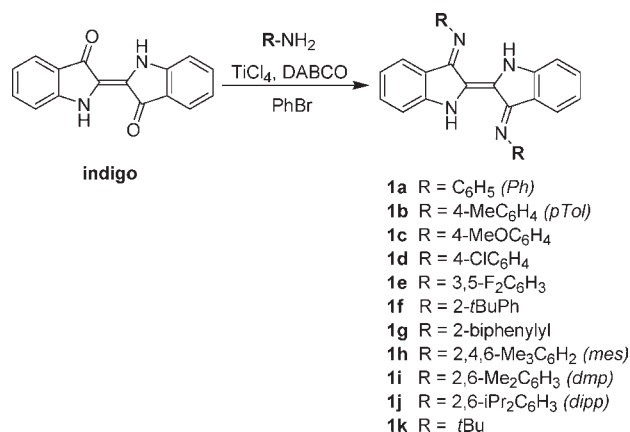


Two recent additions to the bridging RAL family are tetrakis(iminopyracene) **I**²⁴ and the quinone bis(*N*-heterocyclic carbene) ligand **J**.²⁵ Both of these structures have substituents (R) that can be readily installed using efficient synthetic methods and can, in principle, control the steric and electronic environments at the metal(s) to which they coordinate. Examples of such modular systems in bridging RALs, or even binucleating ligands in general, are quite rare. In this context, we recently reported indigo *N,N'*-diarylimines **1**, which, because of the similarity between their two metal binding sites to those of the “NacNac” (β -diketiminato) ligand architecture, we dubbed “Nindigo”.²⁶ Derivatives of **1** can be efficiently made in one step from commercially available reagents, and initial explorations of the coordination chemistry revealed interesting properties such as redox activity and intense near-IR absorption. These properties were revealed to be ligand-centered in origin, which established **1** as a new architecture among bridging RALs. Herein we provide a broader account of the synthesis and properties of ligands and complexes based on **1**.

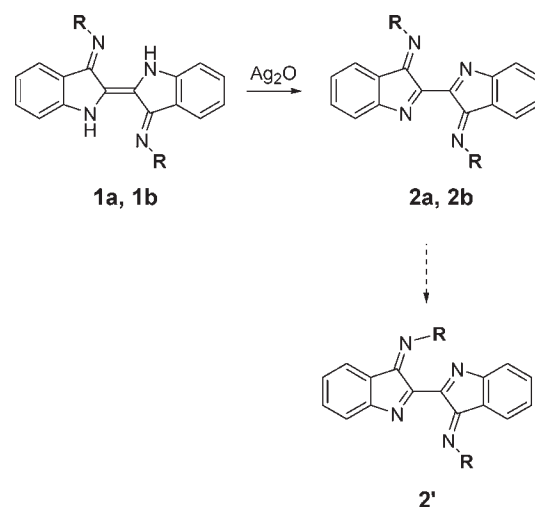


Ligand Syntheses. There are few reports of indigo diimines in the literature. Aryl isonitriles decompose to give diaryl derivatives of **1** in small quantities,²⁷ and multistep, low-yield syntheses have been reported.^{28,29} The first reported Nindigo synthesis involved

Scheme 1



Scheme 2



condensation of the famous dye molecule indigo with aniline.³⁰ Unfortunately, neither we nor others²⁹ could replicate this reaction. However, we found that the protocols developed by Hall et al. for imine condensation of relatively unactivated carbonyl groups³¹ could be adapted for the synthesis of indigo bis(imines). Thus, refluxing a mixture of indigo, primary amine, TiCl₄, and 1,4-diazabicyclo[2.2.2]octane (DABCO) gave very good yields of Nindigo derivatives **1a–1k** (Scheme 1). The use of the high-boiling solvent bromobenzene is required to drive the reaction to completion; corresponding reactions in toluene are much slower and usually lead predominantly to the installation of only one imine. This reaction seems to be quite versatile; Nindigos bearing a wide range of anilines with electron-rich, electron-poor, and bulky substituents can be made, and *tert*-butylamine also reacts with indigo under analogous conditions.

Nindigo derivatives **1a** and **1b** can be oxidized to the corresponding “dehydroNindigo” derivatives **2a** and **2b** (Scheme 2). The dehydro compounds can be isolated as red crystalline solids (see below), but solution characterization consistently reveals the presence of a minor byproduct, not attributable to the parent Nindigo (**1**), that cannot be separated. This new product lacks the symmetry inherent in **2** (and **1**), which leads us to tentatively

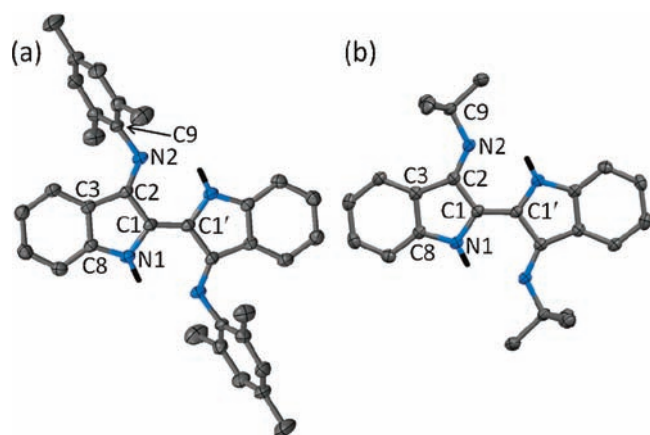


Figure 1. (a) Structure of **1h** (50% probability ellipsoids). Hydrogen atoms except H1A are omitted for clarity. Selected bond lengths (Å) and angles (deg): C1–C1' 1.366(4), C1–N1 1.378(3), C1–C2 1.455(3), C2–N2 1.301(3), C2–C3 1.464(3), C8–N1 1.384(3), C9–N2 1.425(2); C2–N2–C9 121.04(18). (b) Structure of **1k** (50% probability ellipsoids). Hydrogen atoms except H1A are omitted for clarity. Selected bond lengths (Å) and angles (deg): C1–C1' 1.409(3), C1–N1 1.355(2), C1–C2 1.462(2), C2–N2 1.323(2), C2–C3 1.469(2), C8–N1 1.384(2), C9–N2 1.474(2); C2–N2–C9 127.74(14).

suggest **2'**, in which one of the two imines has isomerized from syn to anti, as the minor component.

Nindigo X-ray Structures. We have reported the X-ray structure of dipp-substituted Nindigo **1d**.²⁶ The structures of mesityl and *tert*-butyl derivatives **1h** and **1k**, respectively, are presented in Figure 1. The general structural features of both derivatives are similar to those of **1d**, i.e., the central (C1–C1') bond is rather long for an alkene, and the other C–C and C–N bonds within the core of each molecule also deviate somewhat from the expected values based on the canonical valence-bond representation (Scheme 1). The mesityl substituents of **1h** are twisted by 74° relative to the plane of the Nindigo core, as were the dipp substituents in **1d** (82°).

The structure of the *p*-tolyl derivative **1b**, shown in Figure 2, differs from those of the other Nindigo derivatives. The most glaring distinction is that the two NH protons in **1b** are on the same half of the molecule, with one indole-type proton (on N21) and the other on the exocyclic nitrogen (N22). Moreover, the bond lengths associated with the internal core of the Nindigo are not consistent with the canonical resonance structure depicted for **1**; the tautomeric representation **1b'** more accurately represents the structure of this molecule, in which a C–C single bond links a 3-aminoindole to a dehydroindolimine. Such a tautomer has been proposed to account for unusual features in the vibrational and ¹H NMR spectra of the “parent” Nindigo **1** (R = H).³² The Nindigo core of **1b** remains planar despite the presence of a formal C–C single bond, possibly because of packing effects and/or intramolecular NH–N hydrogen bonds that are likely also present in the other Nindigo derivatives as well as indigo itself.³³ The *p*-tolyl group attached to N12 (on the dehydroindolimine portion of the molecule) is twisted by 73° with respect to the core of the molecule, while the aromatic substituent connected to N22 (i.e., on the 3-aminoindole moiety) is twisted by 54°.

The structure of dehydroNindigo **2a** is shown in Figure 3. The bond alternation patterns in this structure [long central C–C bond, short C–N bonds between the central carbons and the

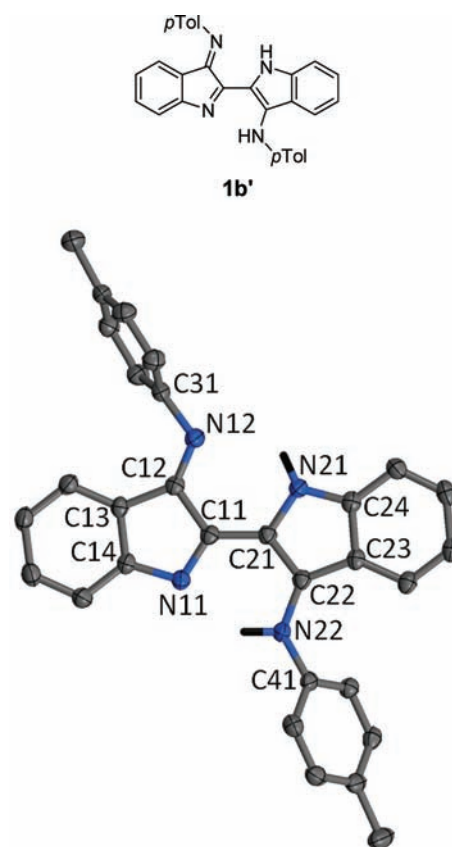


Figure 2. (a) Structure of **1b** (50% probability ellipsoids). Hydrogen atoms except H21N and H22N are omitted for clarity. Selected bond lengths (Å) and angles (deg): C11–C21 1.415(2), C11–C12 1.501(2), C11–C13 1.3208(18), C12–C13 1.475(2), N11–C14 1.4168(18), N12–C12 1.2815(18), N12–C31 1.4248(18), C21–C22 1.397(2), N21–C21 1.3904(18), N21–C24 1.3592(19), N22–C22 1.3666(18), N22–C41 1.4044(19), C22–C23 1.439(2); C11–N11–C14 106.15(12), C12–N12–C31 120.24(13), C21–N21–C24 109.01(12), C22–N22–C41 128.64(13).

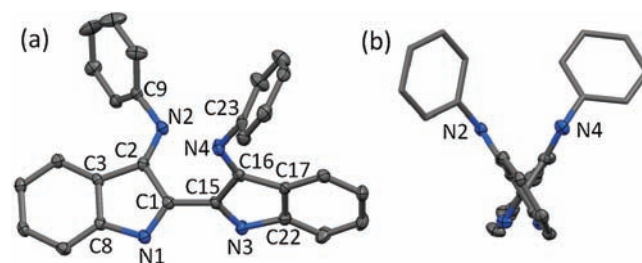


Figure 3. (a) Structure of **2a** (50% probability ellipsoids). Hydrogen atoms are omitted for clarity. Selected bond lengths (Å) and angles (deg): C1–C15 1.4747(18), C1–N1 1.2933(17), C1–C2 1.5003(18), C2–N2 1.2773(17), C2–C3 1.4790(18), C9–N2 1.4216(17), C15–N3 1.2879(17), C15–C16 1.5021(18), C16–N4 1.2714(17), C16–C17 1.4788(18), C22–N3 1.4429(17), C23–N4 1.4250(17); C2–N2–C9 119.09(11), C16–N4–C23 119.93(11). (b) View of the structure of **2a** along the C1–C15 bond.

indole nitrogen atoms, long C1–C2/C15–C16 bonds, and short CN (imine) bonds] confirm the “dehydro” formulation (Scheme 2). The imine bonds both remain syn in the solid state.

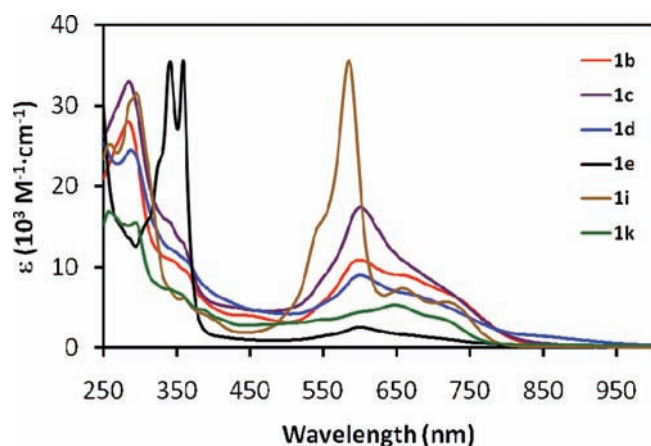


Figure 4. Electronic spectra of selected derivatives of **1**.

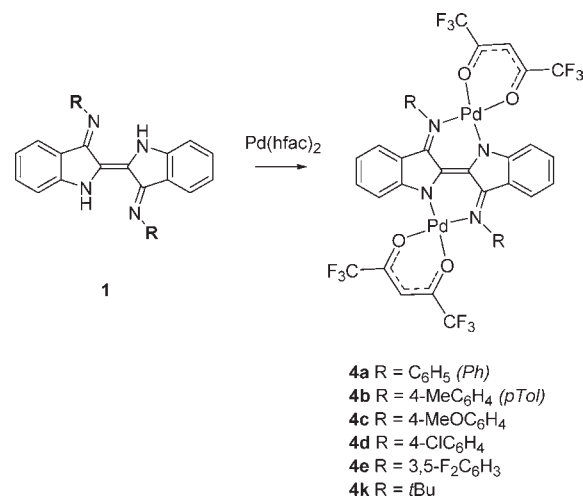
Table 1. Electronic Absorption Maxima Data for Derivatives of **1** near 600 nm

compound	λ_{\max} (nm)	ϵ ($M^{-1} \text{ cm}^{-1}$)
1a	597	11 700
1b	600	10 900
1c	600	17 400
1d	601	8 980
1e	600	2 540
1f	600	20 500
1g	603	10 700
1h	584	26 900
1i	586	35 600
1j	588	33 200
1k		

The two dehydroindole units are twisted relative to one another (about C1–C15) by 113° (with respect to the trans configuration for the parent Nindigo **1a**), and the imine phenyl substituents are twisted by 63° and 85° relative to the half of the indole core to which each is attached.

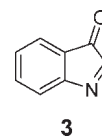
Electronic Spectroscopy of Nindigos. Figure 4 depicts the electronic spectra of representative examples of the Nindigos **1**. We originally reported that **1a**, **1b**, **1i**, and **1j** exhibit concentration-dependent spectra that was attributed to solution aggregation effects.²⁶ We have since found the origin of this observation to be an instrumental artifact; the spectra of all derivatives show no evidence of aggregation within the concentration range of 10^{-4} – 10^{-7} M. The series of Nindigos **1a**–**1k** (Table 1) can be divided into three groups based on qualitative differences in their electronic absorption spectra. The three derivatives with relatively sterically bulky substituents (**1h**, **1i**, and **1j**) all have an intense, narrow absorption band near 585 nm ($\epsilon \sim 3.0 \times 10^4 \text{ M}^{-1} \text{ cm}^{-1}$) superimposed upon a weaker, broader absorption band centered near 650 nm; the latter of these possesses what appears to be some fine structure. The other aryl-substituted Nindigos (**1a**–**1g** and **1k**) share the same basic features as those described above for the bulky derivatives. However, the 585 nm band in the latter is shifted to ~ 600 nm for the other diaryl Nindigo species, and the molar extinction coefficients tend to be significantly lower and substrate-dependent. There appears to be a crude correlation between the

Scheme 3



electron-donating/withdrawing nature of the imine substituent and the extinction coefficient of the 600 nm absorption band; for example, the 4-methoxyphenyl derivative **1c** has the most intense absorption, while the 3,5-difluorophenyl compound **1e** has the least intense. Finally, the spectrum of *tert*-butyl Nindigo **1k**, the only example of a dialkyl Nindigo, has no discernible absorption at 600 nm and instead consists of the broad absorption band centered near 650 nm common to all of the other derivatives. Collectively, the absorption spectra of **1** present some phenomena that as of yet are not understood. For example, the absorption spectrum of indigo consists of a lone band near 600 nm due to a π – π^* transition.³⁴ It is not clear why there are two bands in the Nindigo series, and the near independence of the absorption wavelength, but not the absorption intensity, on the substrate structure also merits further investigation.

The electronic spectra of the (red) dehydroNindigos **2a** and **2b** have their longest wavelength absorption band near 430 nm. The large hypsochromic shifts relative to **1a/1b** are consistent with the loss of donor–acceptor-type conjugation; in fact, the absorption spectra of the dehydroNindigos are quite similar to those of indolone **3** ($\lambda_{\max} = 290$ and 456 nm),³⁵ whose structure is very close to half of the structure of **2a/2b** (with a carbonyl instead of an imine at C3). The spectral similarities between **2** and **3** suggest almost no conjugative overlap between the halves of **2**.



Synthesis of Pd(hfac) Complexes. The coordination chemistry of Nindigos **1a**–**1e** and **1h**–**1k** with palladium has been examined. We previously reported the synthesis of two dipalladium complexes **4a** and **4b** from reactions of the corresponding ligands **1a** or **1b** with Pd(hfac)₂. Other analogous complexes, **4c**, **4d**, and **4e**, can be made using Nindigos that do not possess two ortho substituents (Scheme 3). A dipalladium complex **4k** based on the *tert*-butyl Nindigo was also prepared.

Reactions with the bulkier Nindigo derivatives **1h**, **1i**, and **1j** did not yield isolable dipalladium complexes. We have now found

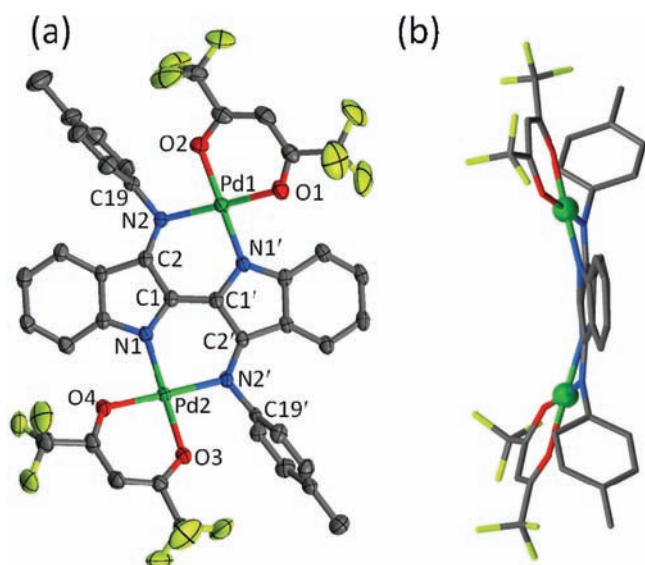
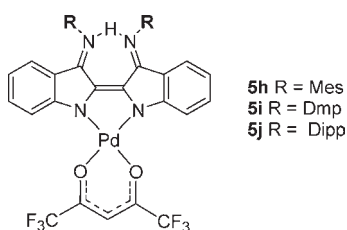


Figure 5. Structure of **4b**: (a) top view and (b) side view (50% probability ellipsoids). Hydrogen atoms are removed for clarity. Selected bond lengths (Å) and angles (deg): C1–N1 1.362(4), C1–C1' 1.368(5), C1–C2 1.445(5), C1'–N1' 1.366(4), C1'–C2' 1.453(5), C2–N2 1.314(5), C2'–N2' 1.315(4), N1–Pd1 1.970(3), N1'–Pd1 1.976(3), N2'–Pd2 1.994(3), N2–Pd1 1.986(3), O1–Pd1 2.028(3), O2–Pd1 2.012(3), O3–Pd2 2.023(3), O4–Pd2 2.018(3); C1–N1–Pd2 123.7(2), C1'–N1'–Pd1 122.9(2), C2'–N2'–Pd2 125.0(2), C2–N2–Pd1 125.0(3), N1'–Pd1–N2 91.55(12), O2–Pd1–O1 89.84(11), N1–Pd1–N2' 90.46(12), O4–Pd2–O3 89.99(11).

that monopalladium complexes **5h**, **5i**, and **5j** can be isolated in modest yields in which the ligand (i) remains monoprotonated and (ii) has isomerized about the central C–C bond to give a *cis*-Nindigo-type structure; the metal is coordinated to the *cis*-Nindigo by two indole nitrogen atoms, and the proton is bound via the imine nitrogen atoms. Minor quantities of dipalladium complexes **4** based on these bulkier ligands can be detected in reaction mixtures by ^{19}F NMR, which suggests that the Pd(hfac) substrate may be able to coordinate to the Nindigo ligands in the imine/amide binding mode (cf. **4**) even when the ligand possesses large imine substituents, but these species are activated toward some process that leads to monopalladium complexes **5**.



X-ray Structures of Nindigo Palladium Complexes. The X-ray structures of **4b** and **4c** are shown in Figures 5 and 6, respectively. The structural features of these complexes are very similar to those of previously reported **4a**.²⁶ In the structure of **4c**, the displacement of the metal atoms from the mean plane of the Nindigo core follows the same pattern as that observed in **4a**; i.e., the two palladium ions are on opposite faces of the ligand plane (Figure 6b). In **4b**, the two metals are on the *same* face, producing

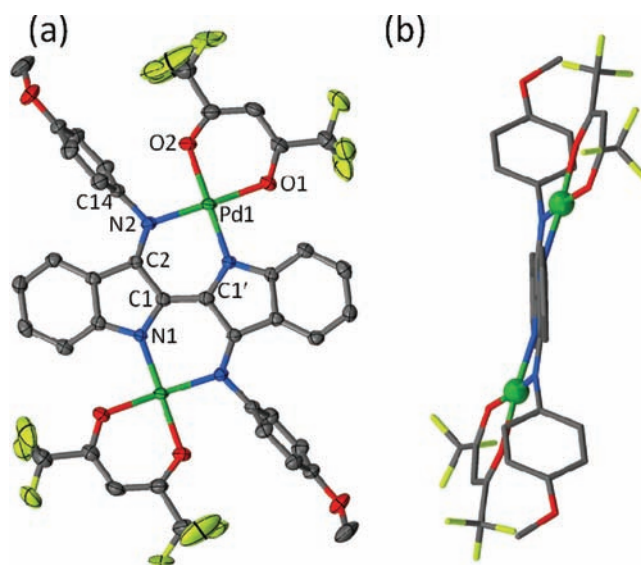


Figure 6. Structure of **4c**: (a) top view and (b) side view (50% probability ellipsoids). Hydrogen atoms are removed for clarity. Selected bond lengths (Å) and angles (deg): C1–N1 1.370(4), C1–C1' 1.379(7), C1–C2 1.454(5), C2–N2' 1.311(4), N1–Pd1 1.990(3), N2–Pd1 1.989(3), O1–Pd1 2.029(2), O2–Pd1 2.043(3); C1–N1–Pd1 123.6(2), C2'–N2–Pd1 125.9(2), N2–Pd1–N1 91.14(11), O1–Pd1–O2 88.31(10).

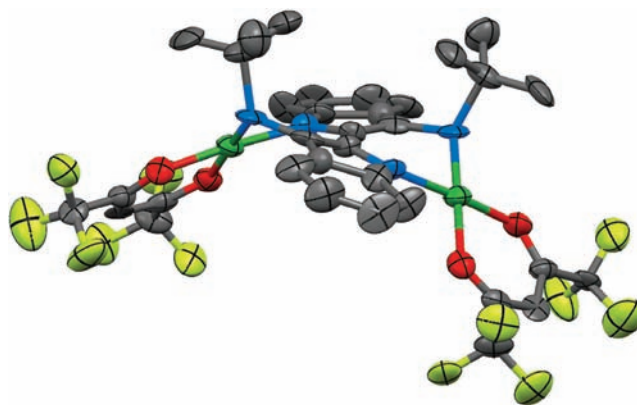


Figure 7. Structure of **4k**. Hydrogen atoms are removed for clarity.

a slightly shorter Pd–Pd separation (6.037 Å) in this structure compared to **4a** (6.167 Å) and **4c** (6.161 Å).

The structure of the dipalladium complex **4k** (Figure 7) based on *tert*-butyl Nindigo is not of sufficient quality to permit any analysis of the bond metrics. However, the structure does confirm the correct atom connectivity and reveals substantial differences in the ligand conformation in comparison to the other dipalladium complexes. The C–N bonds to the *tert*-butyl substituents are not coplanar with the Nindigo core; instead, they are rotated out of the plane such that each *tert*-butyl substituent is wholly on one side of the ligand “plane”. The two Pd(hfac) units are pushed to the opposite side of the ligand, and twisting of the indole-based halves of the ligand core is evident. The strong structural distortions in this compound may provide some insight into the unusual electronic spectrum of this complex relative to the other Nindigo palladium complexes (see below).

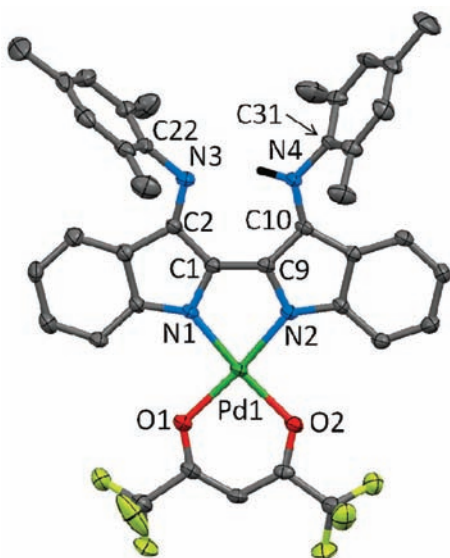


Figure 8. Structure of **5h** (50% probability ellipsoids). Hydrogen atoms other than H(N4) are removed for clarity. Selected bond lengths (Å) and angles (deg): C1–N1 1.356(4), C1–C9 1.387(4), C1–C2 1.467(4), C2–N3 1.309(4), C9–N2 1.383(4), C9–C10 1.440(4), C10–N4 1.333(4), N1–Pd1 1.987(3), N2–Pd1 1.991(2), O1–Pd1 2.022(2), O2–Pd1 2.021(2); C1–N1–Pd1 113.7(2), C9–N2–Pd1 112.69(19), N1–Pd1–N2 80.88(10), O2–Pd1–O1 92.13(9).

The structure of the monopalladium *cis*-indigo **5h** is shown in Figure 8; the structure of the dipp derivative **5j** has also been determined and is analogous to that of **5h** (see the Supporting Information). The structure confirms isomerization of the Nindigo ligand from a *trans*- to *cis*-alkene and the fact that the new ligand binds to palladium via the two indole-type nitrogen atoms. The remaining proton was located on N4 in the solid state, although the solution NMR spectra of this species (as well as the spectra of related compounds **5i** and **5j**) are consistent with a species possessing mirror symmetry, which infers either a symmetric NHN bridge structure or rapid proton transfer between the two sites in solution. The *cis*-Nindigo core remains planar; the mesityl substituents are twisted by 82.5° (on N4) and 70.7° (on N3) relative to this plane. The bond lengths within the Nindigo core are all comparable to the corresponding bonds in the dipalladium complexes **4** of the (*trans*) Nindigos, consistent with the fact that, despite the structural change of the ligand in this structure, the donor–acceptor substitution pattern about the central C–C bond remains the same as that in the original Nindigo structure.

Electronic Spectroscopy of Palladium Complexes. The electronic spectra of representative Nindigo palladium complexes **4a**, **5h**, and **4k** are presented in Figure 9. The spectrum of **4a** is representative of the five dipalladium complexes (**4a**–**4e**) of diaryl Nindigos, all of which have absorption maxima near 920 nm with extinction coefficients on the order of $1.5 \times 10^4 \text{ M}^{-1} \text{ cm}^{-1}$ (Table 2). As discussed previously,²⁶ these are assigned as ligand-based (π – π^*) transitions based on the lack of solvatochromism for any of these derivatives. Thus, metal coordination induces a significant red shift in the low-energy electronic transitions relative to the uncoordinated ligands; analogous spectroscopic behavior has been noted in a few examples of binuclear metal complexes of indigo itself.³⁶ The monopalladium *cis*-Nindigo derivatives **5h**–**5j** also absorb strongly in the near-IR, near 820 nm. The significant outlier

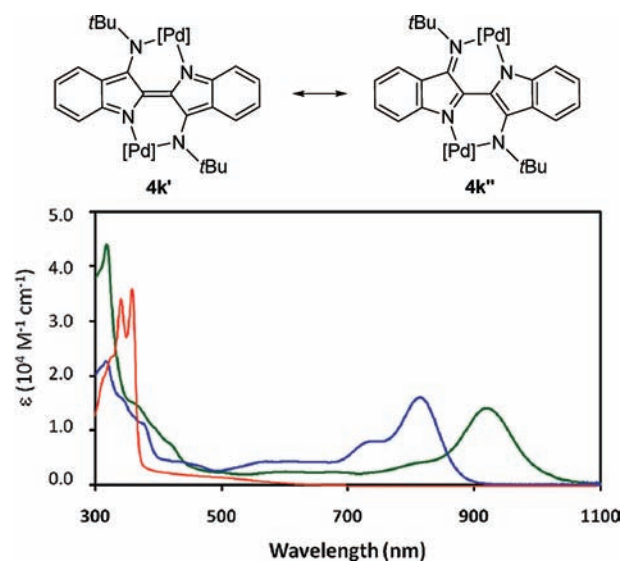


Figure 9. Electronic spectra of Nindigo palladium complexes **4a** (green), **5h** (blue line), and **4k** (red line).

Table 2. Electronic Spectral Data for Nindigo Palladium Complexes

complex	λ_{max} (nm)	ϵ ($\text{M}^{-1} \text{ cm}^{-1}$)
4a	920	14 000
4b	912	18 850
4c	922	16 500
4d	930	12 000
4e	939	13 200
4k	360	49 350
5h	815	14 250
5i	818	15 200
5j	826	16 990

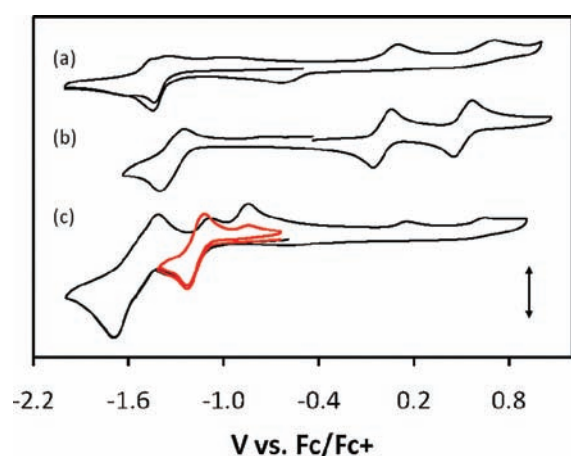
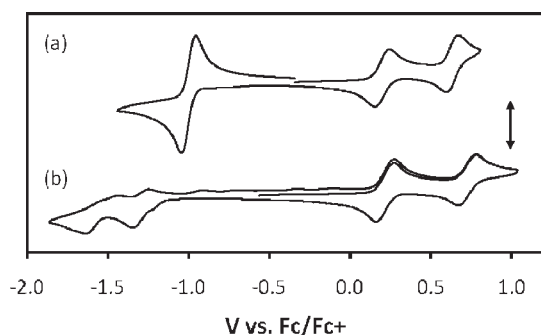
among the Nindigo palladium complexes is the dipalladium complex **4k** based on the *di-tert*-butyl Nindigo. In contrast to all of the other complexes, **4k** does not absorb in the near-IR, instead having an absorption maximum at 360 nm. The gross structural features (cf. Figure 7) indicate a significant perturbation of the ligand structure. In particular, the noncoplanar orientation of the N–C^{*t*Bu} bonds with respect to the Nindigo core suggests alternate formulations of the ligand, e.g., **4k'** and **4k''**, in which one or both of the (formerly) C–N imine bonds are now single bonds. The torsion about the central C–C bond is unlikely to be the cause of the strong blue shift in the electronic spectrum of **4k** relative to other derivatives of **4** because such twisting in N,N'-disubstituted indigo derivatives is known to lead to red shifts in the electronic absorption maxima.³⁷

Cyclic Voltammetry Studies. The redox properties of the Nindigo palladium complexes, as well as a representative Nindigo ligand (**1b**) and its corresponding dehydro compound (**2b**), were probed using cyclic voltammetry techniques; data are presented in Table 3, cyclic voltammograms (CVs) of Nindigo species **1b**, **2b**, and **4b** are presented in Figure 10, and CVs of representative dipalladium Nindigo **4e** and monopalladium *cis*-Nindigo **5j** are shown in Figure 11. Our previous investigations of dipalladium complexes **4a** and **4b** revealed two reversible one-electron oxidations and a quasi-reversible reduction.²⁶ On the

Table 3. Cyclic Voltammetry Data for Palladium Complexes of **1**

complex	reduction	oxidation
4a	-1.21 ^{a,b}	+0.08, +0.57
4b	-1.33 ^{a,b}	+0.05, +0.51
4c	-1.30 ^{a,c}	+0.06, +0.55
4d	-1.14 ^a	+0.14, +0.60
4e	-1.00 ^a	+0.20, +0.60
4k	-1.43	+0.36 ^b
5h	-1.37, -1.70 ^c	+0.16, +0.67 ^b
5i	-1.36 ^b , -1.68 ^c	+0.17, +0.65 ^b
5j	-1.38, -1.74 ^c	+0.19, +0.73 ^b

^a Net two-electron process. ^b Quasi- or semireversible. ^c Irreversible process; only the peak potential is given.

**Figure 10.** CVs of (a) **1b**, (b) **4b**, and (c) **2b** (CH_2Cl_2 solution, ~ 0.1 mM analyte, 0.1 M Bu_4NBF_4 electrolyte, and scan rate 250 mV s^{-1}). The double-headed arrow indicates a 20 μA vertical scale.**Figure 11.** CVs of (a) **4e** and (b) **5j** (CH_2Cl_2 solution, ~ 0.1 mM analyte, 0.1 M Bu_4NBF_4 electrolyte, and scan rate 250 mV s^{-1}). The double-headed arrow indicates a 20 μA vertical scale.

basis of the fact that square-planar palladium(II) complexes are typically not active with respect to electron transfer,³⁸ the redox processes in **4a** and **4b** were assigned as ligand-based in origin. Thus, the first and second oxidation processes correspond to conversion of the (dianionic) Nindigo ligand to a radical anion and then a neutral species, the latter of which is, in fact, the dehydro form of the ligand; i.e., the dication can be described as two $[\text{Pd}(\text{hfac})]^+$ units bound to **2a** or **2b**. As such, we decided to

examine the CV behavior of the dehydroNindigo **2b** as well as the parent ligand **1b**. Although the redox processes seen in the CV of the *p*-tolyl Nindigo ligand **1b** (Figure 10a) are all irreversible, the major processes are nearly coincident with those in the corresponding dipalladium complex **4b**. The CV of the dehydroNindigo **2b** has a quasi-reversible reduction near -1.15 V (vs Fc/Fc^+); sweeps to more negative potentials reveal subsequent irreversible reduction processes. Note that the first reduction process of **2b** should be compared with the second oxidation process in the corresponding dipalladium complex **4b**. Put another way, the reduction of the native dehydroNindigo chromophore in **2b** is shifted by some 1.5 V to higher potential when it is part of **4b**²⁺.

The redox properties of **4b** are representative of the dipalladium complexes **4a–4e** (Table 4). The first and second oxidation processes are separated by approximately 0.5 V in all cases. The substituent effects on the oxidation potentials are modest, but the effects on the reductions are somewhat larger, with respect to not only the reduction potential but also its reversibility. In the case of **4a** and **4b** (Figure 10b), the reduction is partially reversible at scan rates of $100–500$ mV s^{-1} (Figure 10b), whereas for **4c** with a more electron-donating imine substituent, the reduction is totally irreversible. In contrast, the 4-chlorophenyl- and 3,5-difluorophenyl-substituted derivatives **4d** and **4e** (Figure 11a) have reversible reductions that are revealed to be two-electron processes. In fact, all of the reductions within this series (**4a–4e**) were determined to be two-electron processes irrespective of the reversibility of the reduction.

The CVs of the three monopalladium *cis*-Nindigo complexes **5h–5j** also contain multiple redox events. As was found in the dipalladium series, **5h–5j** all have two reversible one-electron oxidation processes; however, their corresponding reductions, the first of which is partially reversible and the second is irreversible, are single-electron processes, in contrast to the two-electron reductions seen for **4a–4e** (Figure 11).

Summary. There are many examples of so-called “privileged” ligands in which substituents can be readily installed and provide a means of control over the steric and electronic properties of the resulting complexes. Many of these are chelating amine/amido-based ligands (e.g., β -diketiminates, amidinates, α -diimines, and diiminopyridines) in which the nitrogen atoms are the donor sites for a metal and the point of substitution. Examples of “tunable” binucleating ligands are extremely rare, despite the demonstrated importance of bridging ligands in mediating interactions between metals in bi- or polymetallic assemblies. In this context, our development of “Nindigo”, essentially two β -diketonate binding sites fused together, has great potential as a bridging ligand architecture that can be readily made with a wide variety of nitrogen substituents. The discovery that these ligands possessing a suite of interesting properties in their resulting complexes such as near-IR absorption and redox activity highlights the fact that, in addition to their possible use in mediating metal–metal communication, these ligands possess significant electronic functionality in their own right. Finally, the imine substituents influence the properties of the ligands and resulting complexes and in some instances even the very nature of the coordination complexes.

EXPERIMENTAL SECTION

General Considerations. All reactions and manipulations were carried out under an argon atmosphere using standard Schlenk or

Table 4. Crystallographic Data

	1b	1g	1k	2a	4b	4c	4k	5h	5j
empirical formula	C ₃₀ H ₂₄ N ₄	C ₃₄ H ₃₂ N ₄	C ₂₄ H ₂₈ N ₄	C ₂₈ H ₁₈ N ₄	C ₄₃ H ₃₁ N ₄ O ₄ F ₁₂ Pd ₂	C ₄₀ H ₂₄ N ₄ O ₄ F ₁₂ Pd ₂	C ₃₄ H ₂₈ N ₄ O ₄ F ₁₂ Pd ₂	C _{40.5} H ₃₈ N ₄ O _{2.5} F ₆ Pd	C ₄₅ H ₄₄ F ₆ N ₄ O ₂ Pd
fw	440.53	496.64	372.50	410.46	1108.52	1097.43	997.40	838.13	893.24
T (K)	173	173	173	90	173	173	173	173	173
wavelength (Å)	0.71073	0.71073	0.71073	0.71073	0.71073	0.71073	0.71073	0.71073	0.71073
cryst syst	triclinic	monoclinic	triclinic	monoclinic	triclinic	triclinic	monoclinic	triclinic	triclinic
space group	$P\bar{1}$	$P2_1/c$	$P2_1/n$	$P2_1/c$	$P\bar{1}$	$P\bar{1}$	$P2/n$	$P\bar{1}$	$P\bar{1}$
a (Å)	9.6208(6)	14.555(3)	6.6748(9)	8.5038(3)	11.2026(10)	5.5243(4)	12.839(2)	12.0116(5)	12.4188(4)
b (Å)	10.5429(6)	7.0908(12)	8.7859(11)	22.0912(7)	13.2615(12)	11.0622(8)	12.383(2)	12.8180(4)	13.3663(4)
c (Å)	12.3563(8)	13.413(3)	17.067(3)	11.1934(4)	13.8826(12)	16.4452(12)	23.962(3)	13.9589(6)	13.5280(4)
α (deg)	110.7996(8)	90	90	90	90.508(5)	97.128(4)	90	112.866(1)	66.8664(3)
β (deg)	100.8409(8)	102.241(8)	100.662(5)	91.511(1)	92.453(5)	96.593(4)	93.044(5)	98.231(1)	78.7331(4)
γ (deg)	100.8226(8)	90	90	90	92.795(5)	102.633(4)	90	107.377(1)	83.0717(4)
V (Å ³)	1105.61(12)	1352.8(5)	983.6(2)	2102.1(1)	2058.0(3)	962.56(12)	3804.3(9)	1805.93(12)	2022.80(11)
Z	2	2	2	4	2	1	2	2	2
μ (cm ⁻¹)	0.79	0.72	0.76	0.78	9.78	10.48	10.47	5.89	5.30
ρ_{calc} (g cm ⁻³)	1.323	1.219	1.258	1.297	1.789	1.893	1.741	1.541	1.467
data collected	8298	11246	5101	28037	43171	28933	28571	13761	17961
unique data	4195	2393	1659	5990	9794	4506	4890	6184	9208
no. of param	317	179	138	289	589	318	496	508	551
GOF	1.025	1.03	1.06	1.02	1.06	1.10	1.08	1.01	1.037
R1	0.0394	0.050	0.039	0.047	0.039	0.041	0.158	0.036	0.0286
wR2	0.1050	0.094	0.082	0.101	0.085	0.078	0.369	0.077	0.0711
CCDC	812586	812587	812588	812589	812590	812591	812592	812593	812594

glovebox techniques unless stated otherwise. Solvents were dried and distilled under argon prior to use. All reagents were purchased from Aldrich and used as received with the exception of DABCO and *p*-toluidine, which were sublimed in vacuo prior to use. NMR spectra were recorded at room temperature on either 300 or 500 MHz instruments. Electronic spectra were recorded on a Perkin-Elmer Lambda 1050 instrument in CH₂Cl₂. Cyclic voltammetry experiments were performed with a Bioanalytical Systems CV50 voltammetric analyzer. Typical electrochemical cells consisted of a three-electrode setup including a glassy carbon working electrode, platinum counter electrode, and silver quasi-reference electrode. Experiments were run at scan rates of 100 or 250 mV s⁻¹. Acetonitrile solutions of the analyte (~1 mM) and electrolyte (0.1 M Bu₄N⁺BF₄⁻) were referenced against an internal standard (~1 mM Fc). Mass spectra were recorded on a Q-TOF II instrument using an electrospray ionization source in the positive mode. *Note*: Derivatives of **1**, **4**, and **5** routinely fail to produce acceptable elemental analyses; carbon analyses are typically low by <3% despite the absence of obvious impurities in the NMR spectra. As such, NMR spectra for all compounds are provided in the Supporting Information.

Indigo Bis(4-Methoxyphenylimine) (1c). A 1.0 M toluene solution of TiCl₄ (4.8 mL, 4.8 mmol) was added dropwise to a bromobenzene (50 mL) solution containing DABCO (2.0 g, 18 mmol) and *p*-anisidine (0.78 g, 6.3 mmol), immediately generating a white vapor and forming a light-green precipitate. After the fuming subsided, indigo (545 mg, 2.1 mmol) was added. The dark-green mixture was heated to reflux overnight. The resulting dark-blue solution was then filtered while still warm, and the filtrate was vacuum distilled to remove bromobenzene. The crude product was dissolved in CH₂Cl₂ (400 mL), washed with water (3 × 200 mL), dried over anhydrous Na₂SO₄, filtered, and evaporated in vacuo. The solid was washed thoroughly with hexanes, yielding **1c** as a dark-purple solid. Yield: 635 mg (64%). ¹H NMR (500 MHz, THF-*d*₈): δ 10.19 (s, 2H), 7.27 (d, *J* = 8.0 Hz, 2H), 7.21 (t, *J* = 8.1 Hz, 2H), 7.14 (d, *J* = 8.9 Hz, 4H), 6.99 (m, 6H), 6.69 (t, *J* = 7.4 Hz, 2H), 3.83 (s, 6H). The solid was not soluble enough to get complete ¹³C NMR data. HRMS. Calcd for C₃₀H₂₅N₄O₂ [(M + H)⁺]: *m/z* 473.1978. Found: *m/z* 473.1938.

Indigo Bis(4-chlorophenylimine) (1d). DABCO (2.0 g, 18 mmol) and *p*-chloroaniline (0.79 g, 6.2 mmol) were dissolved in bromobenzene (50 mL). TiCl₄ (4.8 mL, 1.0 M in toluene, 4.8 mmol) was added dropwise via a syringe, immediately generating a white vapor and forming a light-green precipitate. After the fuming subsided, solid indigo (540 mg, 2.0 mmol) was added. The dark-green mixture was heated to reflux overnight. The resulting dark-blue solution was then filtered hot, and the filtrate was vacuum distilled to remove bromobenzene. The crude product was dissolved in CH₂Cl₂ (400 mL), washed with water (3 × 200 mL), dried over anhydrous Na₂SO₄, filtered, and evaporated in vacuo. The solid was washed thoroughly with hexanes, yielding *p*-chlorophenyl Nindigo as a dark-purple powder. Yield: 630 mg (63%). ¹H NMR (300 MHz, THF-*d*₈): δ 10.21 (s, 2H), 7.41 (d, *J* = 8.7 Hz, 4H), 7.31–7.23 (m, 4H), 7.14 (d, *J* = 8.7 Hz, 4H), 6.93 (d, *J* = 7.8 Hz, 2H), 6.76 (t, *J* = 7.5 Hz, 2H). The solid was not soluble enough to get complete ¹³C NMR data. HRMS. Calcd for C₂₈H₁₉N₄Cl₂ [(M + H)⁺]: *m/z* 481.0987. Found: *m/z* 481.0974.

Indigo Bis(3,5-difluorophenylimine) (1e). A solution of DABCO (2.0 g, 18 mmol) and 3,5-difluoroaniline (0.82 g, 6.3 mmol) was prepared in 50 mL of bromobenzene. TiCl₄ (4.8 mL, 1.0 M in toluene, 4.8 mmol) was added dropwise via a syringe, immediately generating a white vapor and forming a light-green precipitate. Once the fuming had ceased, indigo (545 mg, 2.1 mmol) was added. The dark-green mixture was heated to reflux for 2 days. The dark-brown reaction mixture was cooled to room temperature and then vacuum-distilled to remove bromobenzene. The brown residue was dissolved in 100 mL of acetone and filtered, collecting a dark-green filtrate, which was taken to dryness on the rotary evaporator.

The crude green/brown residue was washed thoroughly with water, followed by dichloromethane (DCM). 3,5-Difluorophenyl Nindigo was collected as a dark-green solid. Yield: 480 mg (48%). ¹H NMR (500 MHz, THF-*d*₈): δ 10.38 (s, 2H), 7.36 (d, *J* = 8.2 Hz, 2H), 7.26 (d, *J* = 7.9 Hz, 2H), 7.11 (t, *J* = 7.6 Hz, 2H), 6.96 (t, *J* = 7.6 Hz, 2H), 6.20–6.12 (m, 6H). ¹³C NMR (125.8 MHz, THF-*d*₈): δ 165.1 (dd, *J* = 242.9 Hz, 15.7), 152.1 (t, *J* = 13.0 Hz), 137.0, 125.8, 125.7, 123.6, 120.5, 119.2, 115.9, 112.4, 97.6 (d, *J* = 28.5 Hz), 93.1 (t, *J* = 26.5 Hz). HRMS. Calcd for C₂₈H₁₇N₄F₄ [(M + H)⁺]: *m/z* 485.1389. Found: *m/z* 485.1387.

Indigo Bis(2-tert-butylphenylimine) (1f). To a bromobenzene (75 mL) solution of DABCO (3.88 g, 34.60 mmol) and 2-*tert*-butylaniline (14.4 mmol, 2.15 g) was added dropwise TiCl₄ (1 M in toluene, 8.63 mmol, 8.63 mL) under nitrogen at 70 °C with rapid stirring. After the complete addition of TiCl₄, indigo (1.51 g, 5.76 mmol) was added and the reaction mixture heated to reflux for 24 h. The reaction mixture was filtered while hot and washed with ether until the washings became clear. The solvent was removed in vacuo, and the crude product was taken up in DCM and extracted with a saturated NaHCO₃ solution. It was then taken up in hot *n*-BuOH and left to cool to room temperature before being put in a freezer for 2 days. The resulting mixture was filtered to give 1.82 g (60.27%) of **1f** as a purple powder. ¹H NMR (300 MHz, CD₂Cl₂, 293 K): δ 1.46 (s, 18H), 6.44 (m, 4H), 6.98 (m, 2H), 7.08 (d, 2H), 7.24 (m, 6H), 7.56 (m, 2H), 10.02 (s, 2H). ¹³C NMR (500 MHz, CD₂Cl₂, 293 K): δ 30.5, 35.7, 113.9, 119.0, 120.4, 122.1, 125.2, 125.9, 127.2, 127.3, 130.9, 131.5, 141.4, 148.0, 150.3, 155.9. HRMS. Calcd for C₃₂H₂₉N₄ [(M + H)⁺]: *m/z* 525.3047. Found: *m/z* 525.3375.

Indigo Bis(2-biphenylimine) (1g). To a bromobenzene (140 mL) solution of DABCO (4.778 g, 42.6 mmol), 2-aminobiphenyl (3.00 g, 17.73 mmol), and indigo (7.1 mmol, 1.860 g) was added dropwise TiCl₄ (1 M in toluene, 16 mmol, 16 mL) under nitrogen at 70 °C with rapid stirring. The reaction mixture was brought to reflux and left to stir for 24 h. The reaction mixture was filtered while hot and washed with ether until the washings became clear. The solvent was removed in vacuo, and the crude product was taken up in DCM and extracted with a saturated NaHCO₃ solution. The solvent was removed and the solid dissolved in chloroform and run through an activated basic alumina column. The solvent was removed, yielding **1g** as a dark solid (247 mg, 6.80%). ¹H NMR (300 MHz, CD₂Cl₂, 293 K): δ 6.773 (t, 2H), 7.00 (d, 2H), 7.08 (d, 2H), 7.31 (m, 14H), 7.47 (m, 6H), 9.69 (s, 2H). ¹³C NMR (500 MHz, CD₂Cl₂, 293 K): δ 115.1, 119.3, 119.6, 121.1, 124.8, 125.1, 127.6, 128.5, 129.8, 131.0, 133.6, 139.8, 150.0. HRMS. Calcd for C₃₂H₂₉N₄ [(M + H)⁺]: *m/z* 565.2392. Found: *m/z* 565.2770.

Indigo Bis(2,4,6-trimethylphenylimine) (1h). DABCO (2.0 g, 18 mmol) and 2,4,6-trimethylaniline (0.88 mL, 6.3 mmol) were dissolved in bromobenzene (50 mL). A solution of TiCl₄ (4.8 mL, 1.0 M in toluene, 4.8 mmol) was added dropwise via a syringe, immediately generating a white vapor and forming a light-green precipitate in a brown solution. Once the fuming had subsided, indigo (545 mg, 2.1 mmol) was added. The dark-green mixture was heated to reflux overnight. The resulting dark-blue solution was filtered while still warm, and the filtrate was vacuum-distilled to remove bromobenzene. The crude product was dissolved in CH₂Cl₂ (400 mL), washed with water (3 × 200 mL), dried over anhydrous Na₂SO₄, filtered, and taken to dryness on the rotary evaporator. The solid was recrystallized from *n*-butanol and washed with a minimum of cold pentane, yielding **1h** as a dark-purple powder. Yield: 430 mg (42%). IR (KBr): 3371, 2939, 2912, 1618, 1570, 1550 cm⁻¹. ¹H NMR (300 MHz, CD₂Cl₂): δ 9.86 (s, 2H), 7.23 (t, *J* = 7.6 Hz, 2H), 7.12 (d, *J* = 8.0 Hz, 2H), 7.00 (s, 4H), 6.62 (t, *J* = 7.5 Hz, 2H), 6.49 (d, *J* = 7.8 Hz, 2H), 2.37 (s, 6H), 2.13 (s, 12H). ¹³C NMR (125.8 MHz, CD₂Cl₂): δ 157.6, 150.3, 144.1, 134.8, 131.8, 130.4, 129.4, 129.2, 124.6, 120.8, 119.5, 114.1, 21.2, 18.4. HRMS. Calcd for C₃₄H₃₃N₄ [(M + H)⁺]: *m/z* 497.2705. Found: *m/z* 497.2569.

Indigo Di-tert-butylimine (1k). A solution of TiCl₄ (4.8 mL, 1.0 M in toluene, 4.8 mmol) was added dropwise to a solution of DABCO (2.0 g, 18 mmol) and *tert*-butylamine (0.66 mL, 6.3 mmol) in 50 mL of

bromobenzene, immediately generating a white vapor and forming an orange/brown solution. After the fuming had subsided, indigo (545 mg, 2.1 mmol) was added. The dark-green mixture was heated to reflux overnight under argon. The resulting dark blue/green solution was then filtered while warm, and the filtrate was vacuum-distilled to remove bromobenzene. The crude product was dissolved in CH_2Cl_2 (400 mL), washed with water (3×200 mL), dried over anhydrous Na_2SO_4 , filtered, and taken to dryness on the rotary evaporator. The solid was washed with a minimum of cold hexanes, yielding **1k** as a dark-purple solid. Yield: 463 mg (60%). ^1H NMR (300 MHz, CD_2Cl_2): δ 9.75 (s, 2H), 7.84 (d, $J = 8.0$ Hz, 2H), 7.34–7.20 (m, 4H), 7.00 (t, $J = 7.3$ Hz, 2H), 1.61 (s, 18H). ^{13}C NMR (125.8 MHz, CD_2Cl_2): δ 153.1, 151.8, 137.5, 129.9, 127.1, 121.3, 119.0, 116.5, 55.5, 30.5. HRMS. Calcd for $\text{C}_{24}\text{H}_{29}\text{N}_4$ [(M + H) $^+$]: m/z 373.2393. Found: m/z 373.2393.

2,2'-Cis(indol-3-phenylimine) (2a). Solid Ag_2O (2 equiv, 210 mg) was added to a solution of **1a** (200 mg, 0.243 mmol) in 80 mL of CH_2Cl_2 , and the reaction mixture was left to stir at room temperature for 24 h. The reaction mixture was filtered and the solvent removed. The remaining solid was recrystallized from hot 1:2 toluene/hexanes to give **2a** as a red solid (106 mg, 50%). ^1H NMR (300 MHz, CD_2Cl_2 , 293 K): δ 7.66 (d, $J = 2$ Hz, 2H), 7.44–7.50 (m, 8H), 7.30 (t, $J = 2$ Hz, 2H), 7.05 (m, 4H), 6.75 (d, $J = 2$ Hz, 2H). ^{13}C NMR (500 MHz, CD_2Cl_2 , 293 K): δ 164.1, 163.4, 158.6, 150.8, 133.79, 130.0, 128.9, 126.2, 123.4, 121.5, 119.2, 118.3. UV–vis (CH_2Cl_2): λ_{max} 343 nm ($\epsilon = 8500 \text{ M}^{-1} \text{ cm}^{-1}$), 437 nm ($\epsilon = 7400 \text{ M}^{-1} \text{ cm}^{-1}$).

2,2'-Bis(indol-3-*p*-tolylimine) (2b). Solid Ag_2O (105 mg, 0.46 mmol) was added to a solution of **1b** (100 mg, 0.227 mmol) in 40 mL of CH_2Cl_2 , and the reaction mixture was left to stir at room temperature for 24 h. The reaction was filtered and the solvent removed. The remaining solid was redissolved in hot 1:2 toluene/hexanes and cooled, giving **2b** as a red solid (53 mg, 50%). ^1H NMR (300 MHz, CD_2Cl_2 , 293 K): δ 7.64 (d, 2H), 7.45 (t, 2H), 7.27 (d, 2H), 7.08 (d, 2H), 6.82–6.95 (m, 8H) 2.40 (s, 6H). ^{13}C NMR (500 MHz, CD_2Cl_2 , 293 K): δ 167.1, 163.9, 163.1, 158.6, 148.2, 136.4, 133.6, 130.5, 128.8, 126.0, 123.2, 121.6, 118.7, 21.3. UV–vis (CH_2Cl_2): λ_{max} 338 nm ($\epsilon = 8600 \text{ M}^{-1} \text{ cm}^{-1}$), 432 nm ($\epsilon = 8700 \text{ M}^{-1} \text{ cm}^{-1}$).

μ -[Indigo bis(4-methoxyphenylimine)]bis(hexafluoroacetylacetonatopalladium) (4c). A solution of $\text{Pd}(\text{hfac})_2$ (330 mg, 0.63 mmol) in THF (25 mL) was added to a solution of **1c** (100 mg, 0.21 mmol) in 25 mL of THF. The dark-green solution was stirred for 30 min and then evaporated to dryness under reduced pressure. The resulting dark-brown/green residue was recrystallized from CH_2Cl_2 /hexanes, giving **4c** as a dark-green solid. Yield: 133 mg (58%). ^1H NMR (300 MHz, CD_2Cl_2): δ 7.21–7.06 (m, 8H), 6.96 (d, $J = 8.9$ Hz, 4H), 6.36 (t, $J = 7.6$ Hz, 2H), 6.18 (s, 2H), 5.85 (d, $J = 8.2$ Hz, 2H), 3.87 (s, 6H). ^{13}C NMR (125.8 MHz, CD_2Cl_2): δ 175.6 (q, $J = 36.4$ Hz), 174.9 (q, $J = 35.7$ Hz), 159.5, 158.6, 156.0, 139.3, 133.2, 133.0, 127.4, 126.4, 121.1, 119.2, 117.3 (q, $J = 284.7$ Hz), 116.7 (q, $J = 285.0$ Hz), 116.7, 115.0, 92.8, 56.2. ^{19}F NMR (282.4 MHz, CD_2Cl_2): δ -74.5, -75.1. HRMS. Calcd for $\text{C}_{40}\text{H}_{25}\text{F}_{12}\text{N}_4\text{O}_6\text{Pd}_2$ [(M + H) $^+$]: m/z 1097.9596. Found: m/z 1097.8584.

μ -[Indigo bis(4-chlorophenylimine)]bis(hexafluoroacetylacetonatopalladium) (4d). A solution of $\text{Pd}(\text{hfac})_2$ (158 mg, 0.30 mmol) in THF (25 mL) was added slowly to a solution of **1d** (58 mg, 0.12 mmol) in 25 mL of THF. The dark-green solution was stirred for 2 h and then taken to dryness on the rotary evaporator. The resulting dark-brown/green residue was recrystallized from CH_2Cl_2 /hexanes, yielding **4d** as a dark-green solid. Yield: 75 mg (57%). ^1H NMR (300 MHz, CD_2Cl_2): δ 7.45 (d, $J = 8.7$ Hz, 4H), 7.24 (d, $J = 8.7$ Hz, 4H), 7.19–6.68 (m, 4H), 6.40 (t, $J = 7.1$ Hz, 4H), 6.20 (s, 2H), 5.87 (d, $J = 8.1$ Hz, 2H). ^{13}C NMR (125.8 MHz, CD_2Cl_2): δ 175.6 (q, $J = 36.1$ Hz), 175.0 (q, $J = 35.6$ Hz), 158.5, 156.1, 144.8, 133.6, 133.4, 133.4, 130.0, 127.9, 126.4, 120.8, 119.5, 117.2 (q, $J = 284.6$ Hz), 116.7 (q, $J = 284.9$ Hz), 116.9, 92.9. ^{19}F NMR (282.4 MHz, CD_2Cl_2): δ -74.4, -75.3. HRMS. Calcd for $\text{C}_{38}\text{H}_{19}\text{Cl}_2\text{F}_{12}\text{N}_4\text{O}_4\text{Pd}_2$ [(M + H) $^+$]: m/z 1105.8607. Found: m/z 1105.8817.

μ -[Indigo bis(3,5-difluorophenylimine)]bis(hexafluoroacetylacetonatopalladium) (4e). A solution of $\text{Pd}(\text{hfac})_2$ (160 mg, 0.30 mmol) in THF (25 mL) was added slowly to a solution of **1e** (50 mg, 0.1 mmol) in 25 mL of THF. The dark-green solution was stirred for 1 h and then taken to dryness on the rotary evaporator. The resulting dark-brown/green residue was recrystallized from CH_2Cl_2 /hexanes, yielding **4e** as a dark-green solid. Yield: 43 mg (38%). ^1H NMR (300 MHz, $\text{THF}-d^8$): δ 7.23 (d, $J = 8.4$ Hz, 2H), 7.19–7.02 (m, 8H), 6.44 (t, $J = 7.6$ Hz, 2H), 6.33 (s, 2H), 6.00 (d, $J = 8.0$ Hz, 2H). ^{13}C NMR (125.8 MHz, $\text{THF}-d^8$): δ 175.8, 175.6, 164.6 (dd, $J = 249.4$ Hz, 14.3), 158.9, 156.9, 149.1 (t, $J = 12.5$ Hz), 134.0, 133.9, 126.4, 120.9, 120.4, 120.2, 118.9, 117.6, 111.0 (d, $J = 27.4$ Hz), 103.8 (t, $J = 25.6$ Hz), 93.2. ^{19}F NMR (282.4 MHz, $\text{THF}-d^8$): δ -74.3, -74.9, -109.9. HRMS. Calcd for $\text{C}_{38}\text{H}_{17}\text{F}_{16}\text{N}_4\text{O}_4\text{Pd}_2$ [(M + H) $^+$]: m/z 1109.9006. Found: m/z 1109.8778.

μ -[Indigo di-*tert*-butylimine]bis(hexafluoroacetylacetonatopalladium) (4k). A solution of $\text{Pd}(\text{hfac})_2$ (420 mg, 0.81 mmol) in THF (25 mL) was added slowly to a solution of **1k** (100 mg, 0.27 mmol) in 25 mL of THF. The dark-green/brown solution was stirred for 30 min and then taken to dryness on the rotary evaporator. The resulting dark residue was recrystallized from *n*-butanol/acetone, yielding **4k** as a dark-red solid. Yield: 41 mg (15%). IR (KBr): 3056, 2973, 1620, 1600, 1458, 1257, 1223, 1154, 1099 cm^{-1} . ^1H NMR (300 MHz, CD_2Cl_2): δ 7.51–7.44 (m, 2H), 7.38–7.31 (m, 2H), 7.05–6.96 (m, 4H), 6.30 (s, 2H), 1.43 (s, 18H). ^{13}C NMR (125.8 MHz, CD_2Cl_2): δ 176.1 (q, $J = 35.6$ Hz), 174.6 (q, $J = 35.5$ Hz), 142.3, 138.4, 126.2, 120.8, 119.4, 117.3, 117.1 (q, $J = 283.8$ Hz), 116.9 (q, $J = 284.8$ Hz), 115.6, 109.6, 92.8, 67.1, 29.3. ^{19}F NMR (282.4 MHz, CD_2Cl_2): δ -74.4, -74.8. HRMS. Calcd for $\text{C}_{34}\text{H}_{25}\text{F}_{12}\text{N}_4\text{O}_4\text{Pd}_2$ [(M + H) $^+$]: m/z 998.0009. Found: m/z 998.0266.

[*cis*-Indigo bis(2,4,6-trimethylphenylimine)]hexafluoroacetylacetonatopalladium (5h). A solution of $\text{Pd}(\text{hfac})_2$ (80 mg, 0.15 mmol) in THF (25 mL) was added to a solution of **1h** (75 mg, 0.15 mmol) in 25 mL of THF. The dark-blue/green mixture was stirred at room temperature for 1 h under argon. After removal of the solvent under reduced pressure, the crude residue was washed with acetone. Recrystallization from DCM/hexanes yielded **5h** as a black solid. Yield: 45 mg (39%). ^1H NMR (300 MHz, CD_2Cl_2): δ 12.37 (s, 1H), 7.53 (d, $J = 8.4$ Hz, 2H), 7.23 (t, $J = 7.8$ Hz, 2H), 6.98 (s, 4H), 6.55 (t, $J = 7.5$ Hz, 2H), 6.40 (s, 1H), 6.34 (d, $J = 7.8$ Hz, 2H), 2.33 (s, 6H), 2.08 (s, 12H). ^{13}C NMR (125.8 MHz, CD_2Cl_2): δ 174.9 (q, $J = 35.4$ Hz), 156.4, 154.5, 144.2, 140.1, 136.8, 133.5, 131.3, 129.8, 125.1, 119.9, 119.6, 117.6 (q, $J = 284.5$ Hz), 114.3, 93.0, 21.3, 18.4. ^{19}F NMR (282.4 MHz, CD_2Cl_2): δ -74.3. HRMS. Calcd for $\text{C}_{39}\text{H}_{32}\text{F}_6\text{N}_4\text{O}_2\text{Pd}$ (M $^+$): m/z 806.1470. Found: m/z 806.1463.

[*cis*-Indigo bis(2,6-dimethylphenylimine)]hexafluoroacetylacetonatopalladium (5i). $\text{Pd}(\text{hfac})_2$ (50.5 mg, 0.1 mmol) was added to a solution of **1i** (45.5 mg, 0.0971 mmol) in CH_2Cl_2 (20 mL), and the reaction was stirred for 1 h. The reaction mixture was then extracted three times with water before the organic layer was dried, resulting in a dark solid. NMR analysis of the crude solid indicated a 6:1 ratio of **5i** and the corresponding dipalladium *trans*-Nindigo complex “**4i**”. The solid was washed repeatedly with MeCN, and the filtrate was reduced in volume to give **5i** as a black solid. ^1H NMR (300 MHz, CD_2Cl_2 , 293 K): δ 2.13 (s, 12H), 6.27 (d, 2H, $J = 7.9$ Hz), 6.41 (s, 14H), 6.54 (tod, 2H, $J = 8.05$ and 0.9 Hz), 7.17 (s, 6H), 7.24 (2H, tod, $J = 7.8$ and 1.2 Hz), 7.54 (d, 2H, $J = 8.52$ Hz), 12.33 (1H, s). ^{13}C NMR (500 MHz, CD_2Cl_2 , 293 K): δ 18.50, 93.02, 114.37, 116.44, 118.70, 120.00, 120.03, 125.00, 127.04, 129.11, 131.66, 133.61, 142.66, 144.27, 154.24, 156.36, 174.75, 175.03. ^{19}F { ^1H } NMR (300 MHz, CD_2Cl_2 , 293 K): δ -74.24 (s). UV–vis (CH_2Cl_2): λ_{max} 818 nm ($\epsilon = 15\,200 \text{ M}^{-1} \text{ cm}^{-1}$). HRMS. Calcd for $\text{C}_{37}\text{H}_{28}\text{F}_6\text{N}_4\text{O}_2\text{Pd}$ (M $^+$): m/z 778.1157. Found: m/z 778.1168.

[*cis*-Indigo bis(2,6-diisopropylphenylimine)]hexafluoroacetylacetonatopalladium (5j). A solution of $\text{Pd}(\text{hfac})_2$ (0.37 mmol, 192.83 mg) in CH_2Cl_2 (10 mL) was added to a solution of **1j** (215 mg, 0.37 mmol) in 25 mL of CH_2Cl_2 , and the blue/green solution was stirred for 1 h. The

crude reaction mixture was then extracted with water (three times), and the solvent was removed. The solid was recrystallized from CH_2Cl_2 /petroleum ether to give **5j** as a dark solid (211 mg, 64%). ^1H NMR (300 MHz, CD_2Cl_2 , 293 K): δ 0.95 (d, 12H, $J = 6.8$ Hz), 1.14 (d, 12H, $J = 6.8$ Hz), 3.06 (septet, 4H, $J = 6.9$ Hz), 6.23 (d, 2H, $J = 7.95$ Hz), 6.40 (s, 1H), 6.48 (2H, t, $J = 7.62$ Hz), 7.28 (m, 8H), 7.54 (d, 2H, $J = 8.46$ Hz), 11.80 (s, 1H). $^{13}\text{C}\{^1\text{H}\}$ NMR (500 MHz, CD_2Cl_2 , 293 K): δ 24.27 (CH_3), 24.45 (CH_3), 29.31, 93.06, 114.35, 119.48, 119.75 (^{13}C), 124.57, 126.28, 127.99, 133.61, 140.60 (^{13}C), 142.42 (^{13}C), 155.49 (^{13}C), 156.40 (^{13}C), 167.44 (^{13}C), 174.23 (^{13}C), 174.73 (^{13}C). $^{19}\text{F}\{^1\text{H}\}$ NMR (300 MHz, CD_2Cl_2 , 293 K): δ -74.25 (s). UV-vis (CH_2Cl_2): λ_{max} 827 nm ($\epsilon = 16\,970\ \text{M}^{-1}\ \text{cm}^{-1}$). HRMS. Calcd for $\text{C}_{45}\text{H}_{44}\text{F}_6\text{N}_4\text{O}_2\text{Pd}$ (M^+): m/z 890.2409. Found: m/z 890.2420.

■ ASSOCIATED CONTENT

S Supporting Information. Crystallographic data files (CIF format), X-ray structure of **5j**, and NMR spectra of all new compounds. This material is available free of charge via the Internet at <http://pubs.acs.org>.

■ AUTHOR INFORMATION

Corresponding Author

*E-mail: rhicks@uvic.ca.

■ ACKNOWLEDGMENT

We thank the Natural Sciences and Engineering Research Council of Canada and the Petroleum Research Fund of the American Chemical Society for support.

■ REFERENCES

- (1) (a) Jorgensen, C. K. *Coord. Chem. Rev.* **1966**, *1*, 164–78. (b) Jorgensen, C. K. *Oxidation Numbers and Oxidation States*; Springer-Verlag: New York, 1969. (c) Ward, M. D.; McCleverty, J. A. *Dalton Trans.* **2002**, 275–288.
- (2) (a) Kaim, W.; Schwederski, B. *Pure Appl. Chem.* **2004**, *76*, 351–364. (b) Kaim, W.; Schwederski, B. *Coord. Chem. Rev.* **2010**, *254*, 1580–1588.
- (3) (a) Wada, T.; Tsuge, K.; Tanaka, K. *Chem. Lett.* **2000**, 910–911. (b) Wada, T.; Tsuge, K.; Tanaka, K. *Angew. Chem., Int. Ed.* **2000**, *39*, 1479–. (c) Wada, T.; Tsuge, K.; Tanaka, K. *Inorg. Chem.* **2001**, *40*, 329–337. (d) Hino, T.; Wada, T.; Fujihara, T.; Tanaka, K. *Chem. Lett.* **2004**, *33*, 1596–1597. (e) Bouwkamp, M. W.; Bowman, A. C.; Lobkovsky, E.; Chirik, P. J. *J. Am. Chem. Soc.* **2006**, *128*, 13340–13341. (f) de Melo, J. S. S.; Rondao, R.; Burrows, H. D.; Melo, M. J.; Navaratnam, S.; Edge, R.; Voss, G. *ChemPhysChem* **2006**, *7*, 2303–2311. (g) Miyazato, Y.; Wada, T.; Tanaka, K. *Bull. Chem. Soc. Jpn.* **2006**, *79*, 745–747. (h) Stanciu, C.; Jones, M. E.; Fanwick, P. E.; Abu-Omar, M. M. *J. Am. Chem. Soc.* **2007**, *129*, 12400–. (i) Blackmore, K. J.; Lal, N.; Ziller, J. W.; Heyduk, A. F. *J. Am. Chem. Soc.* **2008**, *130*, 2728–. (j) Muckerman, J. T.; Polyanysky, D. E.; Wada, T.; Tanaka, K.; Fujita, E. *Inorg. Chem.* **2008**, *47*, 1787–1802. (k) Mukherjee, C.; Pieper, U.; Bothe, E.; Bachler, V.; Bill, E.; Weyhermuller, T.; Chaudhuri, P. *Inorg. Chem.* **2008**, *47*, 8943–8956. (l) Mukherjee, C.; Weyhermuller, T.; Bothe, E.; Chaudhuri, P. *Inorg. Chem.* **2008**, *47*, 11620–11632. (m) Ringenberg, M. R.; Kokatam, S. L.; Heiden, Z. M.; Rauchfuss, T. B. *J. Am. Chem. Soc.* **2008**, *130*, 788–. (n) Rolle, C. J.; Hardcastle, K. I.; Soper, J. D. *Inorg. Chem.* **2008**, *47*, 1892–1894. (o) Zarkesh, R. A.; Ziller, J. W.; Heyduk, A. F. *Angew. Chem., Int. Ed.* **2008**, *47*, 4715–4718. (p) Nguyen, A. L.; Blackmore, K. J.; Carter, S. M.; Zarkesh, R. A.; Heyduk, A. F. *J. Am. Chem. Soc.* **2009**, *131*, 3307–3316. (q) Sylvester, K. T.; Chirik, P. J. *J. Am. Chem. Soc.* **2009**, *131*, 8772–. (r) Lippert, C. A.; Arnstein, S. A.; Sherrill, C. D.; Soper, J. D. *J. Am. Chem. Soc.* **2010**, *132*, 3879–3892.
- (s) Ringenberg, M. R.; Nilges, M. J.; Rauchfuss, T. B.; Wilson, S. R. *Organometallics* **2010**, *29*, 1956–1965. (t) Smith, A. L.; Clapp, L. A.; Hardcastle, K. I.; Soper, J. D. *Polyhedron* **2010**, *29*, 164–169.
- (4) (a) Grutzmacher, H. *Angew. Chem., Int. Ed.* **2008**, *47*, 1814–1818. (b) Chirik, P. J.; Wieghardt, K. *Science* **2010**, *327*, 794–795.
- (5) Ernst, S.; Hanel, P.; Jordanov, J.; Kaim, W.; Kasack, V.; Roth, E. *J. Am. Chem. Soc.* **1989**, *111*, 1733–1738.
- (6) (a) Kasack, V.; Kaim, W.; Binder, H.; Jordanov, J.; Roth, E. *Inorg. Chem.* **1995**, *34*, 1924–1933. (b) Kaim, W.; Lahiri, G. K. *Angew. Chem., Int. Ed.* **2007**, *46*, 1778–1796. (c) Miller, J. S.; Min, K. S. *Angew. Chem., Int. Ed.* **2009**, *48*, 262–272.
- (7) Kato, R. *Bull. Chem. Soc. Jpn.* **2000**, *73*, 515–534.
- (8) Miller, J. S.; Epstein, A. J. *Chem. Commun.* **1998**, 1319–1325.
- (9) Beinert, H.; Holm, R. H.; Munck, E. *Science* **1997**, *277*, 653–659.
- (10) (a) Howard, J. B.; Rees, D. C. *Chem. Rev.* **1996**, *96*, 2965–2982. (b) Lee, S. C.; Holm, R. H. *Chem. Rev.* **2004**, *104*, 1135–1157.
- (11) Brudvig, G. W. *Coord. Chem. Rev.* **2008**, *252*, 231–232.
- (12) Kitagawa, S.; Kawata, S. *Coord. Chem. Rev.* **2002**, *224*, 11–34.
- (13) (a) Frantz, S.; Rall, J.; Hartenbach, I.; Schleid, T.; Zalis, S.; Kaim, W. *Chem.—Eur. J.* **2004**, *10*, 149–154. (b) Kar, S.; Sarkar, B.; Ghumaan, S.; Janardanan, D.; van Slageren, J.; Fiedler, J.; Puranik, V. G.; Sunoj, R. B.; Kaim, W.; Lahiri, G. K. *Chem.—Eur. J.* **2005**, *11*, 4901–4911. (c) Taquet, J. P.; Siri, O.; Braunstein, P.; Welter, R. *Inorg. Chem.* **2006**, *45*, 4668–4676. (d) Braunstein, P.; Bublir, D.; Sarkar, B. *Inorg. Chem.* **2009**, *48*, 2534–2540. (e) Das, H. S.; Das, A. K.; Pattacini, R.; Hubner, R.; Sarkar, B.; Braunstein, P. *Chem. Commun.* **2009**, 4387–4389. (f) Das, H. S.; Weisser, F.; Schweinfurth, D.; Su, C. Y.; Bogani, L.; Fiedler, J.; Sarkar, B. *Chem.—Eur. J.* **2010**, *16*, 2977–2981.
- (14) (a) Dei, A.; Gatteschi, D.; Pardi, L. *Inorg. Chim. Acta* **1991**, *189*, 125–128. (b) Dei, A.; Gatteschi, D.; Pardi, L.; Russo, U. *Inorg. Chem.* **1991**, *30*, 2589–2594. (c) Carbonera, C.; Dei, A.; Letard, J. F.; Sangregorio, C.; Sorace, L. *Angew. Chem., Int. Ed.* **2004**, *43*, 3136–3138. (d) Min, K. S.; Rheingold, A. L.; DiPasquale, A.; Miller, J. S. *Inorg. Chem.* **2006**, *45*, 6135–6137. (e) Tao, J.; Maruyama, H.; Sato, O. *J. Am. Chem. Soc.* **2006**, *128*, 1790–1791. (f) Guo, D.; McCusker, J. K. *Inorg. Chem.* **2007**, *46*, 3257–3274. (g) Min, K. S.; DiPasquale, A. G.; Golen, J. A.; Rheingold, A. L.; Miller, J. S. *J. Am. Chem. Soc.* **2007**, *129*, 2360–2368. (h) Ghumaan, S.; Sarkar, B.; Maji, S.; Puranik, V. G.; Fiedler, J.; Urbanos, F. A.; Jimenez-Aparicio, R.; Kaim, W.; Lahiri, G. K. *Chem.—Eur. J.* **2008**, *14*, 10816–10828. (i) Min, K. S.; DiPasquale, A. G.; Rheingold, A. L.; White, H. S.; Miller, J. S. *J. Am. Chem. Soc.* **2009**, *131*, 6229–6236. (k) Ward, M. D. *Inorg. Chem.* **1996**, *35*, 1712–. (l) Heinze, K.; Huttner, G.; Zsolnai, L.; Jacobi, A.; Schober, P. *Chem.—Eur. J.* **1997**, *3*, 732–743. (m) Heinze, K.; Huttner, G.; Walter, O. *Eur. J. Inorg. Chem.* **1999**, 593–600. (n) Li, B.; Tao, J.; Sun, H. L.; Sato, O.; Huang, R. B.; Zheng, L. S. *Chem. Commun.* **2008**, 2269–2271.
- (15) (a) Keyes, T. E.; Forster, R. J.; Jayaweera, P. M.; Coates, C. G.; McGarvey, J. J.; Vos, J. G. *Inorg. Chem.* **1998**, *37*, 5925–5932. (b) Dinnebier, R.; Lerner, H. W.; Ding, L.; Shankland, K.; David, W. I. F.; Stephens, P. W.; Wagner, M. Z. *Anorg. Allg. Chem.* **2002**, *628*, 310–314. (c) Lerner, H. W.; Margraf, G.; Kretz, T.; Schiemann, O.; Bats, J. W.; Durner, G.; de Biani, F. F.; Zanello, P.; Bolte, M.; Wagner, M. Z. *Naturforsch.* **2006**, *B61*, 252–264. (d) Margraf, G.; Kretz, T.; de Biani, F. F.; Laschi, F.; Losi, S.; Zanello, P.; Bats, J. W.; Wolf, B.; Removic-Langer, K.; Lang, M.; Prokofiev, A.; Assmus, W.; Lerner, H. W.; Wagner, M. *Inorg. Chem.* **2006**, *45*, 1277–1288.
- (16) (a) Caldwell, S. L.; Gilroy, J. B.; Jain, R.; Crawford, E.; Patrick, B. O.; Hicks, R. G. *Can. J. Chem.* **2008**, *86*, 976–981. (b) Pignotti, L. R.; Kongprakaiwoot, N.; Brennessel, W. W.; Baltrusaitis, J.; Luck, R. L.; Urnezisus, E. *J. Organomet. Chem.* **2008**, *693*, 3263–3272.
- (17) (a) Gross, R.; Kaim, W. *Angew. Chem., Int. Ed.* **1987**, *26*, 251–253. (b) Grosslannert, R.; Kaim, W.; Olbrichdeussner, B. *Inorg. Chem.* **1990**, *29*, 5046–5053. (c) Moscherosch, M.; Waldhor, E.; Binder, H.; Kaim, W.; Fiedler, J. *Inorg. Chem.* **1995**, *34*, 4326–4335. (d) Heintz, R. A.; Zhao, H. H.; Xiang, O. Y.; Grandinetti, G.; Cowen, J.; Dunbar, K. R. *Inorg. Chem.* **1999**, *38*, 144–156. (e) Miyasaka, H.; Izawa, T.; Takahashi, N.; Yamashita, M.; Dunbar, K. R. *J. Am. Chem. Soc.* **2006**,

128, 11358–11359. (f) Motokawa, N.; Miyasaka, H.; Yamashita, M.; Dunbar, K. R. *Angew. Chem., Int. Ed.* **2008**, *47*, 7760–7763. (g) Maity, A. N.; Sarkar, B.; Niemeyer, M.; Sieger, M.; Duboc, C.; Zalis, S.; Kaim, W. *Dalton Trans.* **2008**, 5749–5753. (h) Zhao, H. H.; Ota, A.; Prosvirin, A. V.; Reinheimer, E. W.; Dunbar, K. R. *Adv. Mater.* **2010**, *22*, 986–.

(18) (a) Hunig, S.; Erk, P. *Adv. Mater.* **1991**, *3*, 225–236. (b) Hunig, S.; Herberth, E. *Chem. Rev.* **2004**, *104*, 5535–5563.

(19) Kaim, W.; Moscherosch, M. *Coord. Chem. Rev.* **1994**, *129*, 157–193.

(20) Kaim, W. *Coord. Chem. Rev.* **2001**, *219*, 463–488.

(21) (a) Braterman, P. S.; Song, J. I.; Vogler, C.; Kaim, W. *Inorg. Chem.* **1992**, *31*, 222–224. (b) Klein, A.; Kaim, W.; Hornung, F. M.; Fiedler, J.; Zalis, S. *Inorg. Chim. Acta* **1997**, *264*, 269–278. (c) Kaim, W.; Dogan, A.; Wanner, M.; Klein, A.; Tiritiris, I.; Schleid, T.; Stufkens, D. J.; Snoeck, T. L.; McInnes, E. J. L.; Fiedler, J.; Zalis, S. *Inorg. Chem.* **2002**, *41*, 4139–4148.

(22) Kaim, W. *Coord. Chem. Rev.* **2002**, *230*, 127–139.

(23) (a) Chanda, N.; Sarkar, C.; Fiedler, J.; Kaim, W.; Lahiri, G. K. *Dalton Trans.* **2003**, 3550–3555. (b) Maji, S.; Sarkar, B.; Mobin, S. M.; Fiedler, J.; Kaim, W.; Lahiri, G. K. *Dalton Trans.* **2007**, 2411–2418. (c) Kundu, T.; Sarkar, B.; Mondal, T. K.; Fiedler, J.; Mobin, S. M.; Kaim, W.; Lahiri, G. K. *Inorg. Chem.* **2010**, *49*, 6565–6574.

(24) (a) Vasudevan, K. V.; Findlater, M.; Cowley, A. H. *Chem. Commun.* **2008**, 1918–1919. (b) Vasudevan, K. V.; Vargas-Baca, I.; Cowley, A. H. *Angew. Chem., Int. Ed.* **2009**, *48*, 8369–8371.

(25) Tennyson, A. G.; Ono, R. J.; Hudnall, T. W.; Khramov, D. M.; Er, J. A. V.; Kamplain, J. W.; Lynch, V. M.; Sessler, J. L.; Bielawski, C. W. *Chem.—Eur. J.* **2010**, *16*, 304–315.

(26) Oakley, S. R.; Nawn, G.; Waldie, K. M.; MacInnis, T. D.; Patrick, B. O.; Hicks, R. G. *Chem. Commun.* **2010**, *46*, 6753–6755.

(27) (a) Grundmann, C. J. *Chem. Ber.* **1958**, *91*, 1380–1387. (b) Boeyens, J. C. A.; Cook, L. M.; Ding, Y. X.; Fernandes, M. A.; Reid, D. H. *Org. Biomol. Chem.* **2003**, *1*, 2168–2172.

(28) Wenzel, M.; Lehmann, F.; Beckert, R.; Gunther, W.; Gorls, H. *Monatsh. Chem.* **1999**, *130*, 1373–1382.

(29) Kuhn, C.; Beckert, R.; Friedrich, M.; Gorls, H. *J. Heterocycl. Chem.* **2006**, *43*, 1569–1574.

(30) Grandmougin, E.; Dessonlavy, E. *Ber.* **1910**, *42*, 3636–3641.

(31) Hall, H. K.; Padias, A. B.; Williams, P. A.; Gosau, J. M.; Boone, H. W.; Park, D. K. *Macromolecules* **1995**, *28*, 1–8.

(32) (a) Madelung, W. *Ber.* **1913**, *46*, 2259–2264. (b) Madelung, W. *Liebigs Ann. Chem.* **1914**, *405*, 58.

(33) Elsaesser, T.; Kaiser, W.; Luttko, W. *J. Phys. Chem.* **1986**, *90*, 2901–2905.

(34) Miliani, C.; Romani, A.; Favaro, G. *Spectrochim. Acta* **1998**, *A54*, 581–588.

(35) Takekuma, S.; Takekuma, H.; Matsubara, Y.; Inaba, K.; Yoshida, Z. *J. Am. Chem. Soc.* **1994**, *116*, 8849–8850.

(36) (a) Beck, W.; Schmidt, C.; Wienold, R.; Steimann, M.; Wagner, B. *Angew. Chem., Int. Ed.* **1989**, *28*, 1529–1531. (b) Lenz, A.; Schmidt, C.; Lehmann, A.; Wagner, B.; Beck, W. *Z. Naturforsch.* **1997**, *B52*, 474–484.

(37) Miehe, G.; Susse, P.; Kupcik, V.; Egert, E.; Nieger, M.; Kunz, G.; Gerke, R.; Knieriem, B.; Niemeyer, M.; Luttko, W. *Angew. Chem., Int. Ed.* **1991**, *30*, 964–967.

(38) (a) Herebian, D.; Bothe, E.; Neese, F.; Weyhermuller, T.; Wieghardt, K. *J. Am. Chem. Soc.* **2003**, *125*, 9116–9128. (b) Kokatam, S. L.; Chaudhuri, P.; Weyhermuller, T.; Wieghardt, K. *Dalton Trans.* **2007**, 373–378.